Top quark pair production in association with a jet at NLO accuracy with parton showering

Adam Kardos [a,b,*], Costas G. Papadopoulos [a], Zoltán Trócsányi [b,c]

[a] *NCSR Demokritos, Institute of Nuclear Physics, Athens, Greece*
[b] *Institute of Physics, University of Debrecen, H-4010 Debrecen, P.O. Box 105, Hungary*
[c] *Institute of Nuclear Research of the Hungarian Academy of Sciences, Hungary*

ARTICLE INFO

ABSTRACT

We compute the production cross section of a top–antitop pair in association with a jet at hadron colliders at next-to-leading order accuracy matched with parton shower algorithms to make predictions at the hadron level. The parton shower allows for including the decay of the top quarks at the leading order accuracy. We use a framework based on three well established numerical codes, the POWHEG BOX, used for the calculation of the cross section, HELAC, which generates the matrix elements for the Born-level, real emission and the virtual part, and finally a parton shower program, such as PYTHIA or HERWIG, which generate the parton-shower and hadronization.

© 2011 Elsevier B.V. All rights reserved.

1. Introduction

With the startup of the LHC, high energy particle physics entered a new era. At higher energies, measurements with higher precision become available, which poses new demands to the theoretical predictions: the corresponding cross sections are needed beyond leading order (LO) accuracy even for large multiplicity final states. By now standard techniques exist [1,2] for computing the next-to-leading order (NLO) corrections to many phenomenologically interesting processes involving four, or more hard objects (heavy particle or hard jet) in the final state [3–6]. Despite the improved accuracy obtained by computing the cross sections at NLO, there is still a large gap between fixed order theoretical predictions and data collected by the detectors. At fixed order we calculate only hard parton-level processes, while in experiments we observe hadrons. The common practice to fill this gap is the use of parton shower programs [7,8] which also include hadronization models. The advantage of these programs is the generation of unweighted events, which can be utilized for performing the same analysis as on the collected data, allowing for a direct comparison of theory and experiment, or predicting the Standard Model background. However, these programs catch only the important features of small angle radiation off partons, and the distributions

of observable quantities are not expected to give a good description in the regions dominated by large-angle hard emissions.

Until recent years, these two main approaches were used separately for making predictions. Merging NLO computations with parton showers was pioneered by the MCatNLO project [9]. By now all interesting $2 \to 2$ processes are included in the MC@NLO code [10]. Another method for merging NLO computations with parton showers, which produces only positive weight events, was developed in Refs. [11,12]. The latter procedure was later implemented in the POWHEG BOX [13].[1] The POWHEG BOX can almost be considered a black box that requires matrix elements as input and produces unweighted events in the form of Les Houches accord files [14] as output. These events can be processed with the POWHEG BOX for generating the showered events for further analysis.

In this Letter we show the first application to a $2 \to 3$ process of the combination of the POWHEG BOX and the HELAC [2] frameworks for producing showered events of the $t\bar{t}+$ jet final state that can be used to make distributions with correct perturbative expansion up to NLO accuracy. Due to the large collision energy at the LHC, $t\bar{t}$ pairs with large transverse momentum will be copiously produced and the probability for the top quarks to radiate gluons will be sufficiently large to make the $t\bar{t}+$ jet final state measurable with high statistics. Therefore, we make first predictions for such

* Corresponding author at: Institute of Physics, University of Debrecen, H-4010 Debrecen, P.O. Box 105, Hungary.
  E-mail address: kardam@t-online.hu (A. Kardos).

[1] http://powhegbox.mib.infn.it.

Table 1
Flavour structures of the Born processes, $q = u, d, c, s, b$.

$qg \to t\bar{t}q$	$gq \to t\bar{t}q$	$\bar{q}g \to t\bar{t}\bar{q}$	$g\bar{q} \to t\bar{t}\bar{q}$
$gg \to t\bar{t}g$	$q\bar{q} \to t\bar{t}g$	$\bar{q}q \to t\bar{t}g$	

Table 2
Flavour structures of the real-emission processes, $q, q' = u, d, c, s, b$.

$qg \to t\bar{t}qg$	$qq \to t\bar{t}qq$	$q\bar{q} \to t\bar{t}q\bar{q}$
$gq \to t\bar{t}qg$	$\bar{q}\bar{q} \to t\bar{t}\bar{q}\bar{q}$	$\bar{q}q \to t\bar{t}q\bar{q}$
$\bar{q}g \to t\bar{t}\bar{q}g$	$q\bar{q} \to t\bar{t}gg$	$q\bar{q} \to t\bar{t}q'\bar{q}'$
$g\bar{q} \to t\bar{t}\bar{q}g$	$\bar{q}q \to t\bar{t}gg$	$\bar{q}q \to t\bar{t}q'\bar{q}'$
$qq' \to t\bar{t}qq'$	$q\bar{q}' \to t\bar{t}q\bar{q}'$	$gg \to t\bar{t}gg$
$\bar{q}q' \to t\bar{t}\bar{q}q'$	$\bar{q}\bar{q}' \to t\bar{t}\bar{q}\bar{q}'$	$gg \to t\bar{t}q\bar{q}$

events at the TeVatron and the LHC. A more detailed analysis will be presented elsewhere.

2. Method

The cornerstone of our program is the POWHEG BOX [13] framework, that uses the FKS subtraction scheme [15] for the NLO calculation. The POWHEG BOX requires the following input:

- We use flavour structures given in Tables 1 and 2.
- We generate a Born phase space of a massless and two massive momenta using one two-particle invariant and three angles.
- We use HELAC-Dipoles [16] to calculate all the tree-level helicity amplitudes for the Born subprocesses $t\bar{t}ggg \to 0$ and $t\bar{t}q\bar{q}g \to 0$ and the real emission subprocesses $t\bar{t}gggg \to 0$, $t\bar{t}q\bar{q}gg \to 0$ and $t\bar{t}q\bar{q}q'\bar{q}' \to 0$. (We define the corresponding crossing symmetric amplitudes for all incoming momenta and cross into the relevant physical channels.)
- For the colour-correlated squared matrix elements of the Born subprocesses we use HELAC-Dipoles.
- We use the polarization vectors to project the helicity amplitudes to Lorentz basis for writing the spin-correlated squared matrix elements.
- Finally, we obtain the one-loop corrections to the Born subprocesses utilizing the HELAC-Oneloop implementation [2, 17,18] of unitary-based numerical evaluation of one-loop amplitudes [19–26].

With this input POWHEG BOX can be used to generate hadronic events. One may choose any parton shower (PS) Monte Carlo program for generating parton showers, decays of heavy quarks and hadronization. There is one important point in choosing the PS. We generate events with hardest emission measured by the transverse momentum of the emission. If the ordering variable in the shower is different from the transverse momentum of the parton splitting (for instance, the angular ordered showers in HERWIG), then the hardest emission is not necessarily the first one. In such cases the HERWIG discards shower evolutions (vetoed shower) with larger transverse momentum in a subsequent splitting than that in the real emission correction. In addition, a truncated shower simulating wide-angle soft emission before the first emission is also needed in principle, but its effect was found small [27]. As there is no implementation of truncated shower in HERWIG using external LHE event files, the effect of the truncated showers is absent from our predictions.

3. Checks

In order to ensure the correctness of the calculations we performed the following checks relevant to any fixed order calcula-

Table 3
Dependence of the NLO cross section on the technical cut $p_\perp^{\text{t.c.}}$.

$p_\perp^{\text{t.c.}}$ [GeV]	σ^{LO} [pb]	σ^{NLO} [pb]
20	1.583	1.773 ± 0.003
5	1.583	1.780 ± 0.006
1	1.583	1.780 ± 0.010

tion at the NLO accuracy: (i) Compared the cross section at LO to the prediction of the public code MADGRAPH [29] and found complete agreement. (ii) Checked the virtual correction obtained from the HELAC-Oneloop program in several randomly chosen phase space points to that obtained from the implementation in the PowHel (= POWHEG + HELAC) program. (iii) Checked in several randomly chosen phase-space regions that the ratio of the soft- and collinear limits of the real-emission matrix elements and subtractions tend to one in all possible unresolved limits.

There is an important technical issue related to the way of calculation organized in the POWHEG BOX. The selection cuts are applied on the events obtained after hadronization. However, when computing the $t\bar{t}$ + jet production cross section at fixed order, the cuts are applied at the parton level. At LO this means a cut on the transverse momentum of the only massless parton in the final state. At NLO the virtual contribution has the same event configuration as the Born one, but the real emission contribution has two massless partons in the final state, that have to be combined into a jet before the physical cut can be applied. In the POWHEG BOX such a separation of the real and virtual contributions is not possible because the event-generation starts with an underlying Born configuration from which further parton emissions are generated. In order to make the parton-level calculation finite, we can apply a technical cut on the transverse momentum of the single massless parton in the Born configuration. With a given set of selection cuts, one has to check that the chosen technical cut is sufficiently loose such that it does not influence the physical cross section. Typically we find that for jet transverse momentum cuts of several tens of GeV, a several GeV technical cut on the transverse momentum of the massless parton at Born level is sufficiently loose. Another way of treating the same problem, also implemented in the POWHEG BOX, is to use a suppression factor on the underlying Born configuration [28].

4. Comparison to predictions at NLO

The first calculation of the $t\bar{t}$ + jet production cross section was computed by Dittmaier, Uwer and Weinzierl [30,31]. In order to further check our program, we computed the production cross section at NLO accuracy using the same physical parameters as in Ref. [31]. Due to the technical cut mentioned in the previous section, the PowHel framework is not optimal for a fixed-order computation, nevertheless our prediction, $\sigma^{\text{NLO}} = (1.78 \pm 0.01)$ pb is in agreement with the cross section quoted in Ref. [31], $\sigma^{\text{NLO}} = (1.791 \pm 0.001)$ pb, within the uncertainty of our integration. Our prediction is independent of the technical cut below $p_\perp^{\text{t.c.}} \lesssim 5$ GeV as shown in Table 3.

In order to check the predictions obtained with Born-suppression, we computed the distributions published in Ref. [31] at NLO accuracy and we found agreement. Examples are shown in Fig. 1 for the case of the transverse momentum and rapidity distributions of the jet. The lower panels show the ratio of the PowHel-NLO predictions to the predictions of Ref. [31]. The error bars in the lower panel represent the combined statistical uncertainty of the two computations.

We also compared distributions obtained from LHE events, including the first radiation only, to predictions at NLO. For the dis-
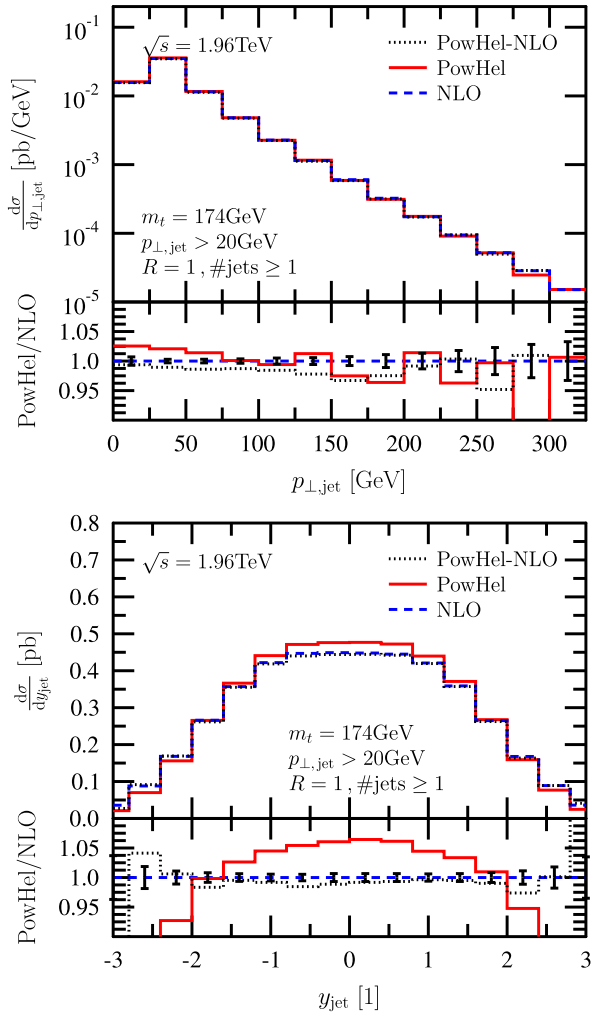
Fig. 1. Transverse momentum and rapidity distributions of the jet.

tributions of the transverse momenta of the jet (see also in Fig. 1) and the top as well as for the rapidity distribution of the top we found agreement. The rapidity distribution of the jet is more central from the LHE events than from NLO.

5. Effects of decays and shower

The production of $t\bar{t}$ + jet final state at the NLO accuracy together with decay of the heavy quarks in the narrow-width approximation (at LO accuracy) has been published recently by Melnikov and Schulze in [32]. In our NLO + PS computation decays of heavy quarks are implemented in the PS, therefore, spin correlations are not included. In contrast, the narrow-width approximation allows for taking into account the spin correlations. Thus, in order to see the effect of the parton shower, we first generated distributions without the shower, but with decays (we just included on-shell decays of t-quarks, and further decays of their decay products, if unstable, turning off any shower and hadronization effect, marked as 'Decay'), then with the full shower Monte Carlo (marked with the name of the SMC). We compared the total cross section as well as several distributions to those predictions made for collisions at the Tevatron, $\sqrt{s} = 1.96$ TeV, valid at the NLO accuracy. We generated two million events with PowHel, which were showered with PYTHIA-6.4.25 [33] and HERWIG-6.5.20 [34] subsequently. For the comparison, we used the semileptonic decay channel and the following parameters and selection cuts from Ref. [32]: (i) mass

of the top quark $m_t = 172$ GeV; all other Standard Model parameters as implemented in the PS programs, (ii) CTEQ6M parton distribution functions, (iii) $k_\perp$-clustering algorithm with $R = 0.5$ and four-momentum recombination scheme [36], (iv) $\mu_R = \mu_F = m_t$, (v) $p_\perp^{\ell^+} > 20$ GeV, (vi) $E_\perp^{\text{miss}} > 20$ GeV, (vii) $p_\perp^j > 20$ GeV, (viii) $|y_j| < 2$, (ix) minimum five jets, and (x) $H_\perp > 220$ GeV, where $H_\perp$ is the scalar sum of transverse momenta in the event, $H_\perp = p_\perp^{\ell^+} + E_\perp^{\text{miss}} + \sum_j p_\perp^j$. In addition, if the final state after these selection cuts contained one or more charged leptons, we rejected the event if the transverse momentum of this lepton was above 20 GeV. This latter requirement is not needed in a fixed order calculation, but necessary in ours to select the semileptonic channel. The technical cut was chosen to $p_\perp^{\text{t.c.}} = 5$ GeV.

The predicted SMC cross sections are very sensitive to the details of the analysis. We kept the leptons and neutral pions stable, while all other particles were allowed to be stable or to decay according to the default implementation in each SMC. Quark masses, as well as W, Z masses and total decay widths, were tuned to the same values in PYTHIA and HERWIG. On the other hand, each of the two codes was allowed to compute autonomously partial branching fractions in different decay channels for all unstable particles and hadrons. Multiparticle interaction effects were neglected (default in HERWIG). Additionally, the intrinsic p_T spreading of valence partons in incoming hadrons in HERWIG was assumed to be 2.5 GeV.

Considering this setup, we always found agreement between PYTHIA and HERWIG predictions within 3%, which is also the effect of including versus neglecting negative weight events in the analysis. For instance, using our selection cuts and taking into account the negative weight events, we obtained the cross sections $\sigma^{\text{PowHel+HERWIG}} = 146.9$ fb and $\sigma^{\text{PowHel+PYTHIA}} = 143.2$ fb, while without the negative weight events, we obtain $\sigma^{\text{PowHel+PYTHIA}} = 147$ fb. The corresponding value for the PowHel + decay case is $\sigma^{\text{PowHel+decay}} = 144.2$ fb (with negative weight events included). These numbers cannot be compared directly to the fixed-order prediction $\sigma^{\text{NLO}} = 33.6$ fb quoted in Ref. [32] for two reasons. On the one hand in Ref. [32] only one lepton family was considered in the decay of the t-quarks, while our prediction contains all three families. We checked that taking into account only one lepton family in the decay we obtain a factor of three reduction of the cross section as expected. On the other hand the authors of Ref. [32] also observed that there is a large contribution to the cross section from the emission of a hard jet from the top decay products (estimated an additional 60% at LO [35]), which is included in our calculation, but not in their value. As this effect is not known at the NLO accuracy, in order to compare only the shapes of distributions with only decays included, we multiply the NLO predictions with $r = \sigma^{\text{PowHel+decay}}/\sigma^{\text{NLO}} = 4.29$ (shown as 'NLO + decay' in Figs. 2 and 3). The lower panels show the ratio of the various predictions to the PowHel + PYTHIA one. In order to exhibit the size of the statistical uncertainty (corresponding to two million LHE events), avoiding at the same time a very confusing plot, we show the uncertainty of only the PowHel + decay prediction with errorbars.

In Fig. 2 we compare the transverse momentum and rapidity distributions of the antilepton at several different levels. We observe on these plots some general features: (i) the two PowHel + SMC predictions are very close except in bins with low statistics; (ii) the PowHel + decay predictions are very close to the NLO ones in the central rapidity region and for the whole $p_\perp$ range. Looking more closely, we find that the spin correlations make the NLO rapidity distribution slightly wider. The addition of the parton shower makes the rapidity distribution a little even more central due to soft leptons emitted by the shower in cen-
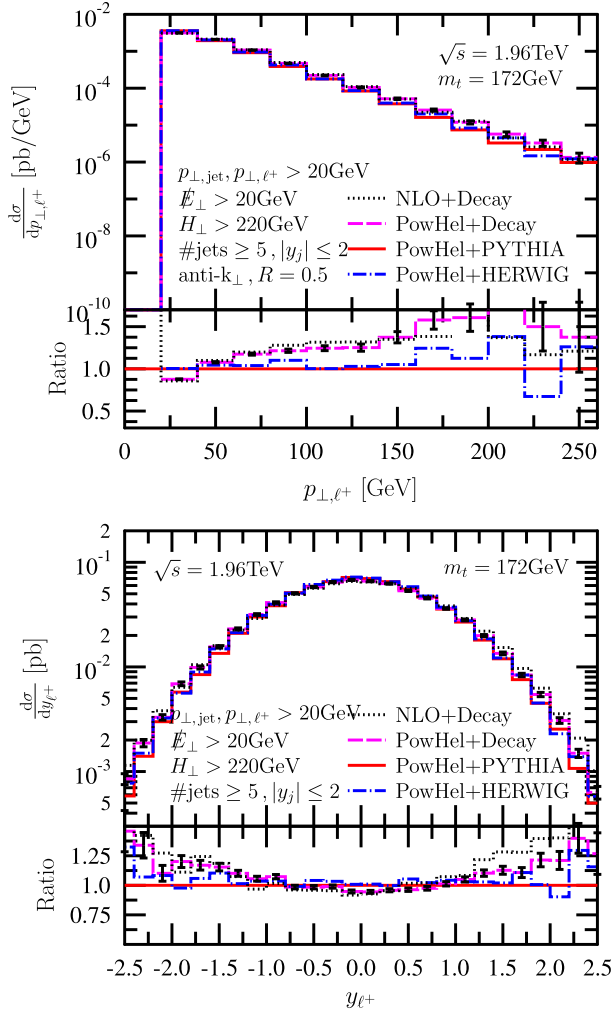
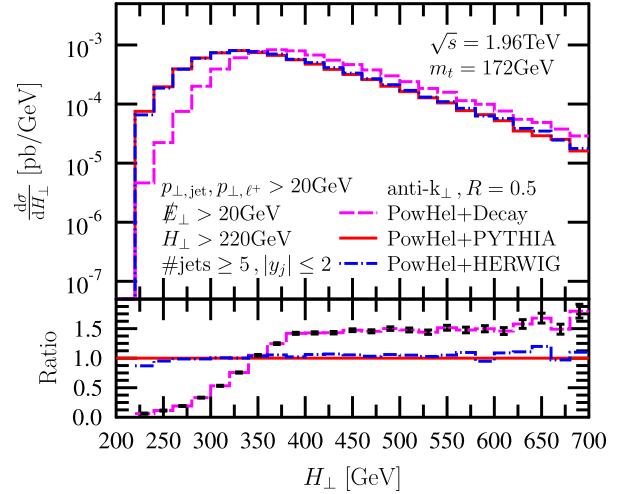**Fig. 2.** Transverse momentum and rapidity distributions of the antilepton.

Fig. 3. Distribution of the scalar sum of transverse momenta.
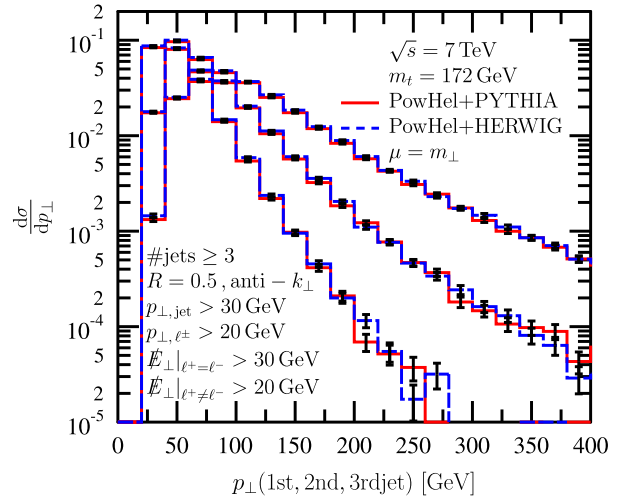
Fig. 4. Transverse momentum distributions of the first, second and third hardest jet.

tral regions. (For jet rapidities, not shown here, the NLO and PowHel + decay predictions coincide, but the shower effect is much more pronounced.) The $p_\perp$-distributions of the leptons becomes much softer for the same reason. The same applies to the $p_\perp$-spectra of the jets.

We find even larger shower effects in the comparison of the $H_\perp$-distributions in Fig. 3 at the decay and SMC levels. The shower makes the distribution softer, readily understood as the effect of unclustered soft hadrons in the event, that appear only in the shower.

6. Predictions for the LHC

We now turn our attention to the LHC and make some predictions for the inclusive $t\bar{t}$ + jet production at the low-energy run, $\sqrt{s} = 7$ TeV in the dileptonic final state channel. We apply the following selection criteria: (i) at least three jets are reconstructed with the anti-$k_\perp$-clustering algorithm with $R = 0.5$ and four-momentum recombination scheme [37], (ii) $p_\perp^j > 30$ GeV, (iii) $|y_j| < 2.5$, (iv) $E_\perp^{\text{miss}} > 30$ GeV for e^+e^- and $\mu^+\mu^-$ pairs, while $E_\perp^{\text{miss}} > 20$ GeV for $e^\pm\mu^\mp$ pairs, (v) $p_\perp^{\ell^-}$, $p_\perp^{\ell^+} > 20$ GeV for exactly one ℓ^+ and one ℓ^-.

For default scales we used two different choices: (i) the mass of the t-quark, m_{t}, and (ii) the transverse mass of the harder top, $\mu_{\text{R}} = \mu_{\text{F}} = m_\perp$, where $m_\perp = \sqrt{m_{\text{t}}^2 + \max\{p_{\text{t}\perp}^2, p_{\bar{\text{t}}\perp}^2\}}$. We expect the

latter scale better interpolates between near-threshold and hard events.

In Fig. 4 we plot the transverse momentum distributions of the hardest, second hardest and third hardest jet. These $p_\perp$ spectra are insensitive to the version of the parton shower within the statistical uncertainty of the computations, which shows that the effect of the missing truncated shower must be small. Also they are rather robust against the choice of the default scale (2–6% variation, not shown here), suggesting small scale dependence in general, but we shall study that in a separate publication. The same features are also true for the rapidity distribution of the antilepton as seen in Fig. 5, where we also exhibited the prediction at the decay level. The lower panel shows the ratios of the predictions to the PowHel + HERWIG case. The error bars represent the statistical uncertainty of the latter only. We find large (almost 20%) and almost uniform effect of the shower and hadronization. In the case of the transverse momentum distribution of the antilepton the various predictions agree over the whole spectrum except that we see a large increase from the decay level to the full SMC at small $p_\perp$, see Fig. 6. We attribute this increase to the numerous secondary antileptons generated in the hadronization phases.

Finally, we plot the invariant mass distribution of the $\ell^+\ell^-$ pairs in Fig. 7. Here again the full SMC predictions are all the same. During hadronization additional (anti)leptons with $p_\perp > 20$ GeV
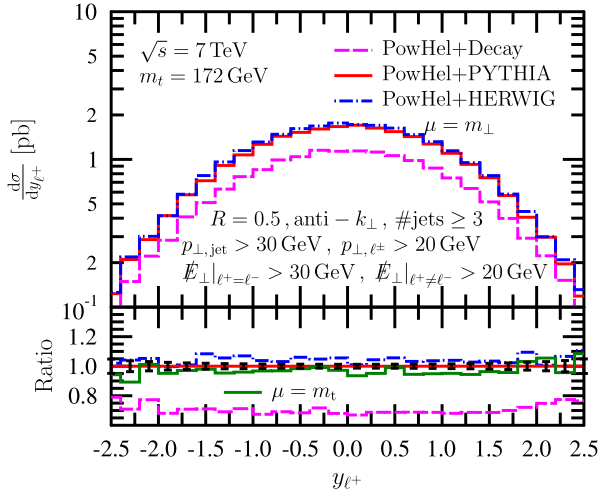
Fig. 5. Rapidity distribution of the antilepton. The lower plot also includes the ratio of the cross section obtained with $\mu = m_t$ to that obtained with $\mu = m_\perp$ (PowHel + PYTHIA).
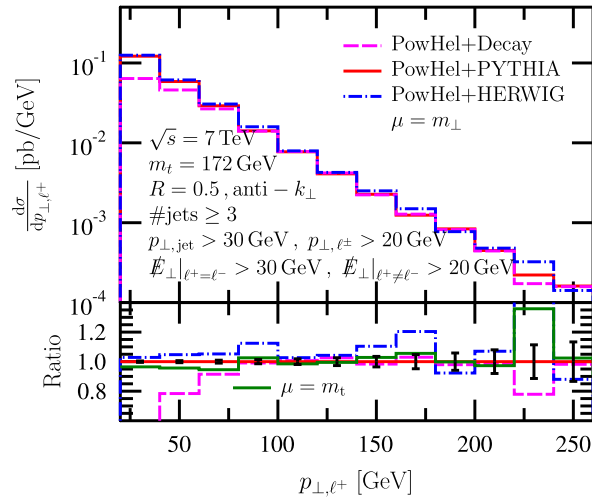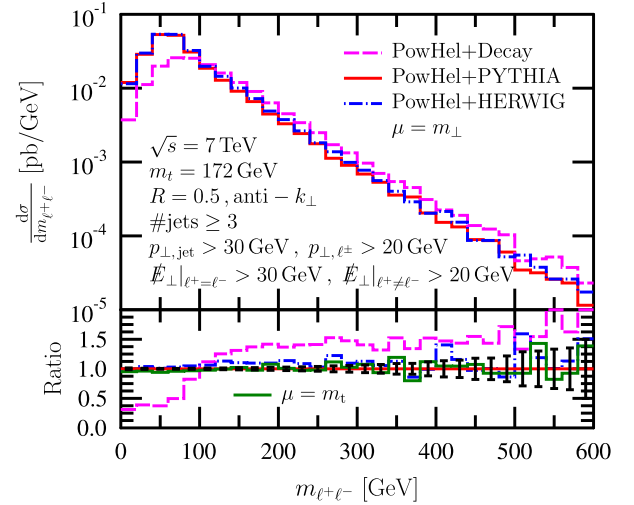

Fig. 6. Transverse momentum distribution of the antilepton. The lower plot also includes the ratio of the cross section obtained with $\mu = m_t$ to that obtained with $\mu = m_\perp$ (PowHel + PYTHIA).

may appear and such events are dropped due to our selection cut (ν), resulting in a softer spectrum.

7. Conclusions

In this Letter we interfaced the POWHEG BOX with the HELAC framework to perform NLO calculations matched with parton showers and hadronization in a quite general and semi-automatic way. The latter means that the necessary ingredients for the POWHEG BOX can be taken from the HELAC framework without any further computations. We presented the feasibility with a non-trivial process, namely inclusive $t\bar{t} +$ jet production and decay, and we found reliable results. We employed decays as implemented in standard PS Monte Carlo programs. We leave the extension to decays included in the hard matrix elements for a future study.

We emphasize that the necessary virtual emission was calculated by a general numerical method which can be used for further processes. Due to the general nature of our framework including further processes is feasible.

Using the PowHel framework we produce several million un-weighted events at the hadron level readily available for analysis. These events can be used to produce distributions that are cor-

Fig. 7. Invariant mass distribution of the lepton–antilepton pair. The lower plot also includes the ratio of the cross section obtained with $\mu = m_t$ to that obtained with $\mu = m_\perp$ (PowHel + PYTHIA).

rect at NLO accuracy when expanded in the strong coupling. Our analyses clearly show the importance of the full SMC. There are certain regions in the phase space, where even a NLO accuracy is insufficient. A singular example is the $H_\perp$ distribution which shows significant softening over the whole kinematic range.

In preparing this Letter we learnt about a similar work in progress by Alioli, Moch and Uwer, presented at the Heavy particles at the LHC workshop, Zurich, 2011.

References

[1] C.F. Berger, et al., Phys. Rev. D 78 (2008) 036003, arXiv:0803.4180.
[2] A. van Hameren, C.G. Papadopoulos, R. Pittau, JHEP 0909 (2009) 106, arXiv:0903.4665.
[3] C.F. Berger, et al., Phys. Rev. D 80 (2009) 074036, arXiv:0907.1984.
[4] G. Bevilacqua, M. Czakon, C.G. Papadopoulos, R. Pittau, M. Worek, JHEP 0909 (2009) 109, arXiv:0907.4723.
[5] G. Bevilacqua, M. Czakon, C.G. Papadopoulos, M. Worek, Phys. Rev. Lett. 104 (2010) 162002, arXiv:1002.4009.
[6] C.F. Berger, et al., Precise predictions for $W + 4$ jet production at the Large Hadron Collider, arXiv:1009.2338.
[7] T. Sjostrand, Comput. Phys. Commun. 82 (1994) 74.
[8] G. Corcella, et al., JHEP 0101 (2001) 010, hep-ph/0011363.
[9] S. Frixione, B.R. Webber, JHEP 0206 (2002) 029, hep-ph/0204244.
[10] S. Frixione, F. Stoeckli, P. Torrielli, B.R. Webber, C.D. White, The MCatNLO 4.0 event generator, arXiv:1010.0819.
[11] P. Nason, JHEP 0411 (2004) 040, hep-ph/0409146.
[12] S. Frixione, P. Nason, C. Oleari, JHEP 0711 (2007) 070, arXiv:0709.2092.
[13] S. Alioli, P. Nason, C. Oleari, E. Re, JHEP 1006 (2010) 043, arXiv:1002.2581.
[14] E. Boos, et al., Generic user process interface for event generators, hep-ph/0109068.
[15] S. Frixione, Z. Kunszt, A. Signer, Nucl. Phys. B 467 (1996) 399, hep-ph/9512328.

[16] M. Czakon, C.G. Papadopoulos, M. Worek, JHEP 0908 (2009) 085, arXiv: 0905.0883.

[17] G. Ossola, C.G. Papadopoulos, R. Pittau, JHEP 0803 (2008) 042, arXiv:0711.3596.

[18] G. Bevilacqua, et al., Nucl. Phys. B (Proc. Suppl.) 205–206 (2010) 211, arXiv:1007.4918.

[19] Z. Bern, L.J. Dixon, D.C. Dunbar, D.A. Kosower, Nucl. Phys. B 435 (1995) 59, hep-ph/9409265.

[20] A. Brandhuber, S. McNamara, B.J. Spence, G. Travaglini, JHEP 0510 (2005) 011, hep-th/0506068.

[21] C. Anastasiou, R. Britto, B. Feng, Z. Kunszt, P. Mastrolia, JHEP 0703 (2007) 111, hep-ph/0612277.

[22] G. Ossola, C.G. Papadopoulos, R. Pittau, Nucl. Phys. B 763 (2007) 147, hep-ph/0609007.

[23] R.K. Ellis, W.T. Giele, Z. Kunszt, JHEP 0803 (2008) 003, arXiv:0708.2398.

[24] Z. Bern, L.J. Dixon, D.A. Kosower, Annals Phys. 322 (2007) 1587, arXiv: 0704.2798.

[25] G. Ossola, C.G. Papadopoulos, R. Pittau, JHEP 0805 (2008) 004, arXiv:0802.1876.

[26] P. Draggiotis, M.V. Garzelli, C.G. Papadopoulos, R. Pittau, JHEP 0904 (2009) 072, arXiv:0903.0356.

[27] O. Latunde-Dada, S. Gieseke, B. Webber, JHEP 0702 (2007) 051, arXiv:hep-ph/0612281.

[28] S. Alioli, P. Nason, C. Oleari, E. Re, JHEP 1101 (2011) 095, arXiv:1009.5594.

[29] J. Alwall, et al., JHEP 0709 (2007) 028, arXiv:0706.2334.

[30] S. Dittmaier, P. Uwer, S. Weinzierl, Phys. Rev. Lett. 98 (2007) 262002, hep-ph/0703120.

[31] S. Dittmaier, P. Uwer, S. Weinzierl, Eur. Phys. J. C 59 (2009) 625, arXiv: 0810.0452.

[32] K. Melnikov, M. Schulze, Nucl. Phys. B 840 (2010) 129, arXiv:1004.3284.

[33] T. Sjostrand, S. Mrenna, P.Z. Skands, JHEP 0605 (2006) 026, hep-ph/0603175.

[34] G. Corcella, et al., HERWIG 6.5 release note, hep-ph/0210213.

[35] M. Schulze, private communication.

[36] S. Catani, Y.L. Dokshitzer, M.H. Seymour, B.R. Webber, Nucl. Phys. B 406 (1993) 187.

[37] M. Cacciari, G.P. Salam, Phys. Lett. B 641 (2006) 57, hep-ph/0512210.